Journal of Materials Chemistry C

Quantitative studies of domain evolution in tetragonal BS-PT ceramics in electric poling and thermal depoling processes

Journal:	*Journal of Materials Chemistry C*
Manuscript ID	TC-ART-02-2019-000748.R1
Article Type:	Paper
Date Submitted by the Author:	08-Mar-2019
Complete List of Authors:	Wu, Jingen; Xi'an Jiaotong University, Gao, Xiangyu; Peking University, Materials Science and Engineering Yu, Yang; Peking University Yang, Jikun; Peking University Chu, Zhaoqiang; Peking University, Bokov, Alexei A.; Simon Fraser University Ye, Zuo-Guang; Simon Fraser University, Chemistry Dong, Shuxiang; Peking University, college of engineering

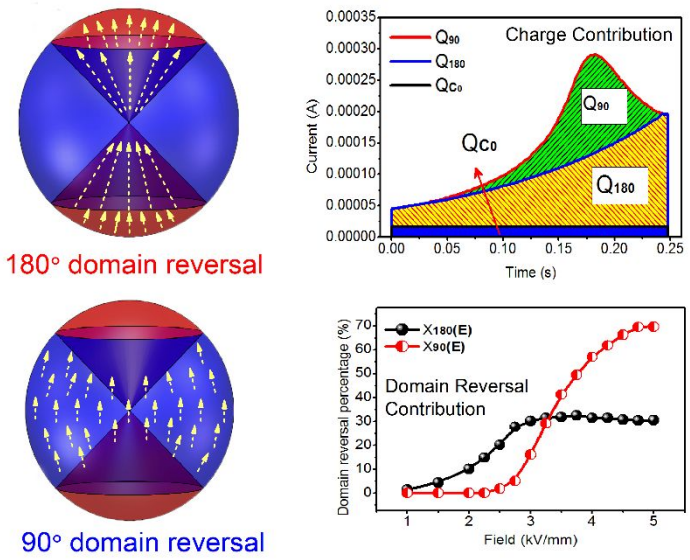

In electric poling process, 180° and 90° domain reversals in tetragonal BS-PT ceramics are quantitively estimated by their charge contributions.

Quantitative studies of domain evolution in tetragonal BS-PT ceramics in electric poling and thermal depoling processes

Jingen Wu[1,3], Xiangyu Gao[1], Yang Yu[1], Jikun Yang[1], Zhaoqiang Chu[1], Alexei A. Bokov[2], Zuo-Guang Ye[2 *] and Shuxiang Dong[1 *]

[1]Department of Materials Science and Engineering, College of Engineering, Peking University, Beijing 100871, People's Republic of China

[2]Department of Chemistry and 4D LABS, Simon Fraser University, Burnaby, British Columbia, V5A 1S6, Canada

[3]Electronic Materials Research Laboratory, Key Laboratory of the Ministry of Education & International Center for Dielectric Research, Xi'an Jiaotong University, Xi'an 710049, China

*Authors to whom correspondence should be addressed. E-mails: zye@sfu.ca, sxdong@pku.edu.cn

Abstract

Bismuth scandate-lead titanate ceramic (abbreviated as BS-PT) is a promising piezoelectric material for high temperature applications because of its excellent piezoelectric performance as well as high Curie temperature. Piezoelectric properties of ferroelectric materials are closely related to microscopic domain structure, however, quantitative analysis on domain evaluation as well as its effect on materials properties in both electric poling and thermal depoling processes is seldom revealed. In this work, we investigate the effects of electric poling and thermal depoling on domain structure and piezoelectric performance in tetragonal BS-PT ceramics. Based on the early work of Uchida and Ikeda, a modified model is developed to quantitively study both 180° and 90° domain reversals during electric poling process. To make clear correlation between domain structure and piezoelectric properties, quantitative estimation of 90° domain reversal in both electric poling and thermal depoling processes is analyzed by XRD method. The present work gives a comprehensive insight into domain evolution of tetragonal BS-PT ceramics, which is also of heuristic significance to other perovskite piezoelectric ceramics.

Keywords: BS-PT ceramics, electric poling, thermal depoling, domain evolution

1. Introduction

The piezoelectricity of ferroelectric ceramics, which results from macroscopic polarization and domain reversal, must be induced by a strong external poling electric field. As ferroelectric ceramics are polycrystalline, their piezoelectric properties are tightly related to the microscopic domain structure. Before electric poling, the spontaneous polarization (P_S), or dipole, is spatially randomly-orientated because of the random grain orientation so that the unpoled material is macroscopically nonpolar. Consequently, ferroelectric ceramics reveal to be non-piezoelectric, with the absence of electromechanical coupling properties or any other piezoelectric performance. Under a poling electric field, the spontaneous polarization (i.e., dipole) in each grain is reoriented to be paralleled to the poling field direction as much as possible, then ferroelectric ceramics become piezoelectric. Crucially, researches on domain structure provide fundamental explanations on physical properties of piezoelectric materials. Hence, the domain evolution and dipole reorientation that account for the dielectric, piezoelectric properties of piezoelectric ceramics are widely investigated in conventional piezoelectric ceramics.[1-9]

Recently, bismuth scandate-lead titanate solid solution ((1-x)$BiScO_3$-$x$$PbTiO_3$, abbreviated as BS-PT) has been continuously drawing intensive research interest since it was first reported by Eitel *et al*.[10] Because of its excellent piezoelectric properties (d_{33} = 460 pC/N) and high Curie temperature (T_C = 450 ºC),[11] BS-PT is a promising piezoelectric material for high temperature applications. It is reported that BS-PT has been successfully used in various high-temperature piezoelectric devices. Piezoelectric motors based on BS-PT ceramics are able to work stably at the temperature as high as 200 ºC.[12-13] A thin ring-shaped BS-PT actuator operating in shear-bending mode can produce an output displacement of 20 μm at 200 ºC.[14] Piezoelectric energy harvesters made of BS-PT piezoelectric ceramics operating in d_{33} or d_{31} mode have been proved to work effectively, converting ambient vibration energy into electric power under high-temperature circumstance.[15-16]

Efforts have also been made to explore the physical mechanism of the high

piezoelectric response and high ferroelectric-transition temperature in BS-PT based piezoelectric materials. Íñiguez *et al.*[17] carried out first-principle study on the (1-*x*)$BiScO_3$-*x*$PbTiO_3$ piezoelectric solid solution and indicated that this material displayed very large structural distortions and polarizations at the MPB (morphotropic phase boundary). Jones *et al.*[18] reported that intrinsic contributions to the electromechanical response were independent of frequency while extrinsic contributions were shown to be dependent upon frequency in *36%*$BiScO_3$-*64%*$PbTiO_3$ composition. Lalitha *et al.*[19] demonstrated a self-consistent set of piezoelectric and structural characterizations that the piezoelectric response of (1-*x*)$PbTiO_3$-*x*$BiScO_3$ ceramic had a direct relationship with the lattice polarizability. Zhao *et al.*[20] studied the high temperature performance of BS-*x*PT-PSN system, and revealed that the mechanisms of its giant piezoelectricity at high temperatures were attributed to the rotation and extension of spontaneous polarization and the MPB-related phase transition. However, there are few researches focusing on the domain evolution in BS-PT ceramics under the conditions of electric poling and thermal depoling. Such issues as the domain evolution due to poling or depoling, the effects of domain configuration on piezoelectric properties, the correlation between phase structure and domain configuration, etc., remain to be solved in BS-PT ceramics, especially in temperature-varying environment.

Previously, based on X-ray diffraction (XRD) method, we proposed the diffraction-plane-transformation (DPT) model to quantitively estimate 90° domain evolution during electric poling process, which well reveals the 90° domain reversal in tetragonal BS-PT piezoelectric ceramics.[21] However, the DPT model cannot reveal 180° domain evolution because 180° domain reversal does not cause any interplanar spacing change that can be detected by X-ray. Accordingly, the quantitative estimation of 180° domain evolution cannot be realized by XRD method. In this work, by introducing Gaussian probability distribution function of domain reversal, a modified Uchida-Ikeda model is built for tetragonal BS-PT ceramics. 180° and 90° domain reversals in tetragonal BS-PT ceramics are distinguished according to their charge contributions. The contributions of 180° and 90° domain reversals to polarization

charge under a poling field are quantitatively estimated by the modified model. Meanwhile, the domain structure evolution of tetragonal BS-PT piezoelectric ceramics under both electric poling and thermal depoling is investigated using scanning electron microscope (SEM) and high-resolution X-ray diffraction method. The percentage of 90° domain reversal is quantitively estimated based on the XRD profiles, and correspondingly, the relationship between 90° domain reversal and piezoelectric properties is clearly established.

2. Experiment

In our experiments, *0.367*$BiScO_3$-*0.633*$PbTiO_3$ is found to be a tetragonal composition that close to the morphotropic phase boundary (MPB), and we use this composition to study 180° and 90° domain reversals. Samples of *0.367*$BiScO_3$-*0.633*$PbTiO_3$ piezoelectric ceramic were prepared by conventional solid-state synthesis,[22] using the following raw materials: PbO (99 % purity; Xilong Chemical Co., Ltd., Shantou, China), TiO_2 (98.5 % purity; Beijing Chemical Works, Beijing, China), Bi_2O_3 (99 % purity; Sinopharm Chemical Reagent Co., Ltd., Beijing, China), and Sc_2O_3 (99.99 % purity; Rare-chem Hi-tech Co., Ltd., Huizhou, China). Stoichiometric mixtures were ball milled for 24 hours with ethanol as the milling medium. The milled powder was subsequently dried at 80 °C and then calcined at 840 °C for 4 hours. The calcined powder was compacted into piece under an uniaxial press of 10 MPa, using PVA as a binder. After burning off PVA, green compacts were sintered at 1080 °C for 3 hours, embedded in the calcined powder having the same composition. The sintered pellets were polished and electroded with a postfire silver paste at 650 °C for 0.5 hours. To measure piezoelectricity, all ceramic samples were poled in a silicone oil bath at 120 °C under a DC electric field for 20 minutes. The resultant specimens were aged in air for 24 hours prior to any electrical measurements.

The piezoelectric constant (d_{33}) of specimens was measured using a quasi-static d_{33} meter (ZJ-3D; Institute of Acoustics, Beijing, China). The electromechanical coupling factors were calculated based on the resonance method using an impedance

analyzer (4294A; Agilent Technologies).[23] A chemical etching technique was used to observe the domain structure. The BS-PT ceramic samples were polished and etched at room temperature in a mixed aqueous solution of HCl/HF acids.[24] The surface microstructure of sintered pellets was imaged by scanning electron microscopy (SEM; S-4800, Hitachi, Tokyo, Japan). The ferroelectric properties (including switching current) of the samples were tested with a TF Analyzer 2000 Measurement System (aixACCT Systems GmbH, Germany). To avoid the residual stress in near-surface region that produced by mechanical polishing, the electrode on the ceramic sample was removed by etching in HCl/HF acids, and then high-resolution X-ray diffraction (XRD) measurements with a monochromatic *Cu-Kα1* radiation (PANalytical X'Pert Powder, Netherland) were carried out to determine the crystalline phase and domain texture of resultant ceramic samples. All the samples were measured by slow scanning at 0.25°/min in the diffraction angle (2θ) range of 20° to 60° with a resolution of 0.003°.

3. Results and Discussion

3.1. Domain evolution during electric poling

During electric poling process, both 180° dipole reversal and 90° dipole reversal in tetragonal BS-PT ceramics will be induced by the poling electric field, as schematically shown in Fig. 1. 180° and 90° reversed domains are the microscopic regions that respectively contain numerous 180° reversed dipoles and 90° reversed dipoles. Accompanied by domain reversal, the macroscopic polarization will be induced. Therefore, the electric displacement (D_3), which practically equals to the macroscopic polarization in ferroelectric materials, can be calculated by using the following equation:

$$D_3 = \varepsilon_0 \varepsilon_r E_3 + (P_{180} + P_{90}), \quad (1)$$

where ε_0 is the permittivity of vacuum, ε_r is the relative dielectric constant, E_3 is the external poling electric field, P_{180} and P_{90} are the polarization contributions of the reversible 180° and 90° domains, respectively. P_{180} and P_{90} can be estimated by the following equations:

$$P_{180} = \eta_{180}(E_3) N_{180}\, p_{180}, \quad (2)$$

$$P_{90} = \eta_{90}(E_3) N_{90}\, p_{90}, \quad (3)$$

where N_{180} and N_{90} are respectively the total quantities of 180° and 90° dipoles in reversible 180° and 90° domains. $\eta_{180}(E_3)$ and $\eta_{90}(E_3)$ are the percentages of the reversed 180° and 90° dipoles, respectively, and they are functions of the applied poling electric field E_3. p_{180} and p_{90} are the average polarization contributions of 180° and 90° dipole reversals, respectively.

It is well known that dipoles in an unpoled piezoelectric ceramic are randomly orientated, thus a virtual intact sphere that includes dipoles of all possible orientations can be used to represent the initial distribution of dipoles.[25-26] Previously, Uchida and Ikeda proposed such a sphere model for estimating the electrostriction and polarization in perovskite-type ferroelectric ceramics under an arbitrary biasing field.[27] As for an unpoled isotropic tetragonal BS-PT ceramic, all the possible dipoles are distributed in either 180° domain or 90° domain, and their space orientations are also regarded as an uniform distribution in the sphere (Fig. 1). Therefore, on the aspect of quantity, 180° and 90° reversed dipoles have the same volume density. According to this sphere model, only the dipoles distributing within the red spatial region (denoted as V_{180}), as presented in Fig. 1(a-i), can produce 180° reversal during electric poling. Similarly, only the dipoles distributing within the blue spatial region (denoted as V_{90}) can produce 90° reversal, see Fig. 1(b-i). Then, N_{180} and N_{90} can be estimated by V_{180} and V_{90}, and for the reason that dipoles have uniform distribution in the sphere, we have $N_{180}/N_{90} \approx V_{180}/V_{90}$. From the sectional view of sphere model, it is also deduced that the boundary angle between red region and blue region is around 45°, where domain switching of tetragonal phase is energetically unfavorable.[28-29]

However, Uchida and Ikeda's sphere model did not present a quantitative estimation of 180° or 90° domain reversal under a poling electric field. Domain reversal in ferroelectric ceramics is a sophisticated process, which can be regarded as the competition results of poling electric field versus elastic distortion, steric hindrance, point defects, etc. As for a specific dipole reversal, it is impossible to judge when and how its reversal is completed because of its complicated ambient conditions. To make

matters worse, there are innumerable kinds of such dipole reversals in a ferroelectric ceramic. Here, we introduce a Gauss probability distribution function to describe these innumerable dipole reversals. The quantitative estimation of 180° and 90° domain reversals is accordingly given, which is confirmed by poling-induced charge measurements.

Under a poling electric field, only dipoles within the red spatial region of the sphere mode may produce 180° domain reversal (Fig. 1(a-iii)). P_S is the spontaneous polarization of each dipole, and φ is the angle of dipole orientation relative to the vertical center line, i.e., the poling direction. Thus, $2P_S cos\varphi$ is the polarization variation of each 180° reversed dipole. Assuming that the domain reversal (in a large quantity) obeys statistical distribution, we can introduce an orientation state distribution function, i.e., Gaussian probability distribution function $f_{180}(\varphi)_I$ and $f_{180}(\varphi)_{II}$ about φ, to describe the 180° domain reversal possibility during electric poling. Then the real polarization contribution of each 180° reversed dipole should be $2P_S cos\varphi f_{180}(\varphi)_I$, or $2P_S cos\varphi f_{180}(\varphi)_{II}$. Therefore, the average polarization contribution of each 180° dipole reversal can be estimated by the following three equations:

$$p_{180} = \frac{\int_0^{\frac{\pi}{4}} 2P_S cos\varphi f_{180}(\varphi)_I dV_{180}}{\int_0^{\frac{\pi}{4}} dV_{180}}, \tag{4}$$

$$f_{180}(\varphi)_I = \frac{1}{\sqrt{2\pi}\delta_{180}} \exp\left(-\frac{\varphi^2}{2\delta_{180}^2}\right),\ \varphi \in [0, \frac{\pi}{4}]$$

$$\text{and } f_{180}(\varphi)_{II} = \frac{1}{\sqrt{2\pi}\delta_{180}} \exp\left(-\frac{(\varphi-\pi)^2}{2\delta_{180}^2}\right), \varphi \in [\frac{3\pi}{4}, \pi] \tag{5}$$

$$dV_{180} = 2\pi r^2 sin\varphi d\varphi dr, \quad \varphi \in [0, \frac{\pi}{4}] \cup [\frac{3\pi}{4}, \pi], \tag{6}$$

where dV_{180} is the volume element of 180° domain, and the total volume of red region can be calculated as $V_{180} = 2\int_0^{\frac{\pi}{4}} dV_{180} = (4 - 2\sqrt{2})\pi r^3/3$, where r is the radius of the hypothetical sphere, see Fig. 1(a-iii). δ_{180} is the standard deviation about φ in 180° dipole reversal, which can be numerically determined to be less than 0.25 by integrating Eq.(5) ($\int_0^{\pi/4} f_{180}(\varphi)_I d\varphi + \int_{3\pi/4}^{\pi} f_{180}(\varphi)_{II} d\varphi = 1$).

Analogously, for each 90° reversed dipole, its polarization contribution can be calculated as $\Delta p_{90} = P_S(sin\varphi - \cos\varphi) f_{90}(\varphi)$, and the average polarization contribution

of each 90° dipole reversal can also be estimated by the following three equations, see Fig. 1(b-iii):

$$p_{90} = \frac{\int_{\frac{\pi}{4}}^{\frac{3\pi}{4}} P_S(sin\varphi - cos\varphi) f_{90}(\varphi) dV_{90}}{\int_{\frac{\pi}{4}}^{\frac{3\pi}{4}} dV_{90}}, \quad (7)$$

$$f_{90}(\varphi) = \frac{1}{\sqrt{2\pi}\delta_{90}} \exp\left(-\frac{(\varphi - \frac{\pi}{2})^2}{2\delta_{90}^2}\right), \quad (8)$$

$$dV_{90} = 2\pi r^2 sin\varphi d\varphi dr, \quad \varphi \in [\tfrac{\pi}{4}, \tfrac{3\pi}{4}], \quad (9)$$

where $f_{90}(\varphi)$ is the Gaussian probability distribution function to describe the possibility of 90° dipole reversal, φ is the angle of dipole orientation relative to the vertical center line, dV_{90} is the volume element of 90° reversed domain. The total volume of V_{90} can be calculated as $2\sqrt{2}\pi r^3/3$, and δ_{90} is the standard deviation about φ in 90° dipole reversal, which also can be numerically determined to be less than 0.25 by the similar method of 180° dipole reversal.

According to equation (6) and equation (9), 180° reversed dipole and 90° reversed dipole are distributed in different regions, i.e., 180° domain and 90° domain. As for 180° reversed dipole and 90° reversed dipole, their orientation angles (i.e., φ) are in the ranges of $[0, \frac{\pi}{4}] \cup [\frac{3\pi}{4}, \pi]$ and $[\frac{\pi}{4}, \frac{3\pi}{4}]$, respectively. Thus, both 180° domain and 90° domain can switch across a broad range of spatial orientation angle. Based on numerical simulation, p_{180}/p_{90} is found to be close to 1, implying that single dipole reversal which either belongs to 180° domain or 90° domain averagely has the same contribution to macroscopic polarization.

To further investigate the polarization contribution of 180° and 90° domain reversals, the switching current of BS-PT ceramic samples was measured, on account of switching current is directly related to domain reversal.[30] Based on equation (1), we can obtain the poling-induced macroscopic charge using the following equations:

$$Q_3 = \oint(\varepsilon_0\varepsilon_r E_3 + P_{180} + P_{90})dS = Q_{C_0} + Q_{180} + Q_{90}, \quad (10\text{-a})$$

$$Q_{C_0} = \oint(\varepsilon_0\varepsilon_r E_3)dS = C_0 V, \quad (10\text{-b})$$

$$Q_{180} = \oint P_{180} dS, \quad (10\text{-c})$$

$$Q_{90} = \oint P_{90} dS, \quad (10\text{-d})$$

where Q_3 is the total induced charge along the poling direction of BS-PT ceramic sample, S is the area of electrode, C_0 is the capacitance of the initially unpoled BS-PT ceramic sample, and V is the applied voltage. From equation (10-a), it can be deduced that the poling-induced charge includes three parts: (i) the capacitance stored charge Q_{C_0}, (ii) 180° domain reversal induced charge Q_{180} and (iii) 90° domain reversal induced charge Q_{90}, which means that both 180° and 90° domain reversals induce additional charge during electric poling process.

The charge stored in capacitance C_0 is calculated by $Q_{C_0} = C_0 V$, and the corresponding charging current, which can be calculated by $\frac{dQ_{C_0}}{dt} = C_0 \frac{dV(t)}{dt}$, is found to be a constant because the applied voltage V increases linearly with respect to time, as shown in Fig. 2(a). The current induced by 180° domain reversal is experimentally found to be an exponential function of time, shown in Fig. 2(b). And the current induced by 90° domain reversal reveals a peak distribution around coercive filed E_c, shown in Fig. 2(c). Based on the measured switching currents and their time dependence, we can obtain the domain reversal induced charge, i.e., Q_{90} and Q_{180}, according to $Q = \int I dt$.

Fig. 2(a-i), 2(b-i) and 2(c-i) respectively present the measured switching currents under low (0.25kV/mm), medium (2kV/mm) and high (5kV/mm) poling electric fields. The applied voltage is set as triangle wave so that $\frac{dV(t)}{dt}$ can be a constant to simplify the capacitance calculation. It is revealed that there is no domain reversal occurring under low poling field, therefore, the measured switching current exhibits the behavior of capacitance (C_0) charging. Thus, the stored charge totally comes from the charging capacitance, i.e., Q_{C_0} has a nearly 100% contribution to the stored charge in the sample under low poling electric field, demonstrating that no domain reversal occurs under low poling electric field, see Fig. 2(a-ii). Under a medium poling electric field of 2 kV/mm, both capacitance C_0 and 180° domain reversal contribute to the stored charge, and the 180° domain reversal induced current can be well fitted by an exponential equation. The charge induced by 180°domain reversal takes up ~76% of the total charge, see Fig. 2(b-ii). When the poling electric field increases to a sufficiently high strength, 90° domain reversal is found to have a dominant contribution to the stored charge, because

the switching current curve presents a prominent peak-shape distribution around the coercive field where 90° domain reversal occurs. The charge contributions of capacitance C_0, 180° domain reversal and 90° domain reversal are respectively ~7%, ~27% and ~66% at the poling electric field of 5 kV/mm, see Fig. 2(c-ii). These results reveal that 180° and 90° domain reversals are strongly dependent on poling field. It is also noted that 180° domain reversal exhibits a fast increase with respect to poling field, while 90° domain reversal occurs only when the poling field is higher than a threshold value, and becomes more prominent than 180° domain reversal under an adequately high poling electric field.

Fig. 3(a) shows the switching current as a function of time under different poling electric field. It is revealed that the switching current increases slowly under low poling electric field, where 180° domain reversal is dominant. The increase of switching current speeds up as the poling electric field further increases, gradually appearing a peak value. This phenomenon shows that 90° domain reversal will not occur until the poling electric field exceeds a threshold value known as coercive field. Thereafter, 90° domain reversal becomes more dominant than 180° domain reversal in the contribution to switching current. Fig. 3(b) shows the time dependence of the total induced charge under different poling fields. Clearly, the induced charge is strongly related to the poling electric field. As the poling field increases, the induced charge increases faster with respect to time, and then gradually trends to saturation, implying that the domain reversals at high electric field tend to become steady. Fig. 3(c) schematically shows the calculation of induced charge that contributed from capacitance charging (Q_{C_0}), 180° domain reversal (Q_{180}) and 90°domain reversal (Q_{90}) under the electric poling field of 3 kV/mm. The whole area as shown in Fig. 3(c) represents the total induced charge. To separate the overlapped switching currents that resulted from 90° and 180° domain reversals, an exponential fitting function is used to describe the 180° domain related switching current. By excluding 180° domain switching current and Q_{C_0} charging current, the 90° domain switching current can be obtained.

Then we can give a quantitative estimation of 180° and 90° domain reversals based on the poling-induced charge. It has been aforementioned that p_{180}/p_{90} is close to 1,

meaning that single 180° or 90° dipole reversal almost has the same contribution to macroscopic polarization during electric poling. According to the equations (2), equations (3), equation (10-c) and equation (10-d), we have:

$$\frac{Q_{180}}{Q_{90}} = \frac{P_{180}}{P_{90}} = \frac{\eta_{180}(E_3)N_{180}}{\eta_{90}(E_3)N_{90}}, \quad (11)$$

$$\eta_{180}(E_3) = Q_{180}(E_3)/Q_{180}^{\text{saturation}}, \quad (12\text{-a})$$

$$\eta_{90}(E_3) = Q_{90}(E_3)/Q_{90}^{\text{saturation}}, \quad (12\text{-b})$$

where $Q_{180}^{\text{saturation}}$ and $Q_{90}^{\text{saturation}}$ are respectively the saturation charge induced by 180° domain reversal and 90° domain reversal. In our experiment, $Q_{180}^{\text{saturation}}$ and $Q_{90}^{\text{saturation}}$ are acquired from the BS-PT ceramic sample poled under 5 kV/mm. $Q_{180}(E_3)$ and $Q_{90}(E_3)$ are acquired from the samples that poled under electric fields below 5 kV/mm. In a sufficiently poled sample, we have $\eta_{180}(E_3) \approx 1$, $\eta_{90}(E_3) \approx 1$ and $\frac{Q_{180}}{Q_{90}} = \frac{N_{180}}{N_{90}} \approx \frac{V_{180}}{V_{90}}$. It is interesting to note that $Q_{180}^{\text{saturation}}/Q_{90}^{\text{saturation}} \approx 0.43$ is in well accordance with $V_{180}/V_{90} \approx 0.414$, which further confirms that the quantitative estimation of domain reversal based on the poling-induced charge is reasonable.

Thus, the contributions of 180° and 90° domain reversals to the total domain reversals under different poling field E_3, i.e., $X_{180}(E_3)$ and $X_{90}(E_3)$, can be respectively estimated by their normalized charge contributions:

$$X_{180}(E_3) = Q_{180}(E_3)/(Q_{180}^{\text{saturation}} + Q_{90}^{\text{saturation}}), \quad (13\text{-a})$$

$$X_{90}(E_3) = Q_{90}(E_3)/(Q_{180}^{\text{saturation}} + Q_{90}^{\text{saturation}}). \quad (13\text{-b})$$

The normalized charge contributions with respect to the external poling field E_3 are presented in Fig. 3(d). It is found that both 180° and 90° domain reversals exhibit a non-linear increase and gradually reach saturation with the increase of poling electric field. However, compared with 90° domain reversal, 180° domain reversal exhibits a faster saturation tendency with respect to poling field. 180° domain reversal reaches saturation at 3 kV/mm, while the other saturates at 5 kV/mm, which indicates that 90° domain is much more difficult to reverse than that of 180° domain due to its large strain distortion. Our experimental results also show that the contributions of 180° and 90° domain reversals respectively account for ~29% and ~71% of the total domain reversals in sufficiently poled tetragonal BS-PT ceramic samples. Similar results were also found in PZT bulk ceramics, in which 90° domain reversal contributes by 80% to the total

reversed domains.[31]

3.2. Contribution of 90° domain reversal to piezoelectricity

As shown in the SEM images of Fig. 4, both electric poling and thermal depoling have direct effects on domain configuration. From Fig. 4(a)-(c), it can be seen that distinct domain structures gradually grow up when poling electric field increases. As for an unpoled sample, its domain structure is disordered because of the randomly orientated spontaneous polarization. While under a medium poling electric field of 2 kV/mm, the domain configuration is ordered to some extent. After sufficiently poled at 4 kV/mm, the domain structure becomes fully ordered, see Fig. 4(c). Fig. 4(d), (e) and (f) respectively show the microtopographies of the ceramic samples that annealed for 1 hour at 200 ℃, 400 ℃ and 450 ℃. Before annealing, these ceramic samples have been sufficiently poled. It is found that the domain structure in the sample annealed at 200 ℃ almost remains the same as that of a sufficiently poled sample, implying that thermal depolarization rarely happens at or below 200 ℃. When the annealing temperature increases to 400 ℃, the ordered domain structure partly disappears due to thermal depoling effect, see Fig. 4(e). It is further found that the ordered domain structure totally disappears when the annealing temperature increases to 450 ℃, as shown in Fig. 4(f). This is ascribed to the fact that ferroelectric-transition temperature, i.e., Curie temperature, can induce domain extinction because of the disappeared spontaneous polarization.

Even though the surface topography reveals an intuitionistic view of the domain evolution under electric poling and thermal depoling, we still cannot present a quantitative analysis of domain evolution and its effect on piezoelectric properties. Additionally, we are unable to make quantitative analysis on the whole domain reversals, for the reason that among 90° and 180° domain reversals, only 90° domain reversal is detectable by XRD measurement. Nevertheless, considering that 90° domain reversal makes the greatest contribution (up to ~71%) to the total domain reversal during poling process, it is reasonably deduced that 90° domain reversal makes a

dominant contribution to the piezoelectric properties. Therefore, from the view of 90° domain reversal, we quantitatively reveal the correlation between domain structure and piezoelectric properties.

The quantitative estimation of 90° domain reversal is based on the diffraction-plane-transformation model.[21] According to this model, the intensity of {111} diffraction peak remains unchanged whether tetragonal piezoelectric ceramics is poled or depoled, therefore, it can be used as the intensity reference to calculate the 90° domain reversal percentage. The 90° domain reversal percentage in poling process can be estimated by the intensity variation of {200} diffraction peak as:

$$N_{pole} = \frac{R_{200} - R'_{200}}{R_{200}} , \quad (14)$$

Where N_{pole} is the 90° domain reversal percentage during poling, R_{200} is the intensity ratio of I_{200}/I_{111} in the unpoled ceramic sample, and R'_{200} is the intensity ratio of I'_{200}/I'_{111} in a poled ceramic sample.

Conversely, the 90° domain reversal percentage in depoling process can be estimated by the intensity variation of {002} diffraction peak as:

$$N_{depole} = \frac{R_{002} - R'_{002}}{R_{002}} , \quad (15)$$

Where N_{depole} is the 90° domain reversal percentage during depoling, R_{002} is the intensity ratio of I_{002}/I_{111} in a sufficiently poled ceramic sample, and R'_{002} is the intensity ratio of I'_{002}/I'_{111} in a depolarized ceramic sample.

In tetragonal ferroelectric ceramics, 90° domain can be classified into two kinds, i.e., *c*-domain and *a*-domain, which are defined according to their orientations. *c*-domain refers to the domain that parallels to the poling direction, and *a*-domain is the horizontal domain which is perpendicular to the poling direction.[32-33] On account of the relation between domain volume and diffraction intensity, both *c*-domain and *a*-domain can be revealed by diffraction intensity. The domain volume of *a*-domain can be reflected by {200} diffraction intensity, while the domain volume of *c*-domain can be reflected by {002} diffraction intensity.[34] Under a poling field, *a*-domain will transform into *c*-domain via 90° domain reversal, which is reflected by the intensity decrease of {200} diffraction peak as well as the intensity increase of {002} diffraction

peak. Vice versa, *c*-domain will transform into *a*-domain via 90° domain reversal in depoling process, which is also reflected by the intensity variations of {002} and {200} diffraction peaks. The intensity variations of {002} and {200} diffraction peaks in poling and depoling processes are experimentally revealed by XRD measurement. Fig. 5 and Fig. 6 respectively show the XRD profiles for ceramic samples poled and depoled under different conditions. As can be seen in Fig. 5, the intensity of {200} diffraction peak gradually decreases when poling electric field increases, which indicates that the volume of *a*-domain decreases during poling. Similarly, in Fig. 6, the intensity of the {002} diffraction peak decreases, demonstrating that the volume of *c*-domain decreases during depoling. Based on the XRD profiles and equations (14)-(15), we can quantitively estimate the 90° domain reversal percentage in both poling and depoling processes.

Fig. 7(a), (b), (c) and (d) respectively show the variations of piezoelectric constant d_{33}, permittivity ε_r, electromechanical coupling factor k_p and 90° domain reversal percentage as a function of poling field and annealing temperature. Strong consistency is found among these material properties. Both of them initially increase with the increasing poling field, and reach their saturated values when poling electric field increases to ~3 kV/mm, indicating that the ceramic sample gradually reaches a sufficiently polarized state. The 90° domain reversal percentage N_{pole} increases with the increase of poling electric field, and it finally reaches ~53.8% at the field of 4 kV/mm. Similar 90° domain reversal percentage in tetragonal PZT piezoelectric ceramic under electric poling was also found in previously reported works.[35-36]

As equally important as the poling process, depolarization of piezoelectric ceramics is also widely investigated.[37-39] The conventional methods that investigate depolarization can be classified into two kinds, i.e., *in situ* and *ex situ*.[40] Recently, an *in situ* techniques is developed to reveal the real-time high temperature performance and depolarization characteristics of piezoelectric ceramics.[41] Differently, we investigate the depolarization of BS-PT ceramics in an *ex situ* way. After sufficiently poled and anterior to any characterization of depolarization, BS-PT ceramic samples are annealed for 1 hour under different temperatures. Here, it must be noted that silver

electrode of ceramic sample has to be removed before the sample is thermally depoled, because the electrode may have effects on the depolarization, such as the thermal expansion mismatch between ceramic sample and electrode. Fig. 7(a), (b), (c) and (d) also show the variations of d_{33}, ε_r, k_p and N_{depole} as a function of annealing temperature. During thermal depoling, it is found that almost no depolarization occurs when annealing temperature is below 200 ºC, convinced by the phenomena that d_{33}, ε_r, k_p and N_{depole} stably maintain their initial value. However, once the annealing temperature increases to 300 ºC or above, a remarkable depolarization is triggered. N_{depole} increases with the increase of annealing temperature, and it becomes dominant (~34.9%) at the ferroelectric-phase transition temperature of 450 ºC. Concurrently, d_{33}, ε_r and k_p also reveal a fast decline when annealing temperature exceeds 300 ºC. From the view of 90° domain reversal, it can be demonstrably deduced that depolarization is almost negligible at temperatures below 200 °C, because N_{depole} is below 5%. This is in well accordance with the material properties that piezoelectric constant d_{33} also remains as high as 95% of its initial value. Hence, it is concluded that the highest safety working temperature for BS-PT piezoelectric ceramics is near the half of Curie temperature (~450 ºC), which coincides well with our previous results.[15, 42] The quantitative study of 90° domain reversal provide us with a more direct perspective to see that BS-PT ceramic has a good thermal stability. The high temperature resistance of BS-PT ceramic proves its promising prospect in the high-temperature applications for aerospace, automotive industries and oil drilling, etc.

4. Conclusions

In the present work, domain evolution of tetragonal BS-PT piezoelectric ceramics, as well as its effects on domain microtopography and piezoelectric properties, are systematically investigated in electric poling and thermal depoling processes. By introducing Gaussian probability distribution function of domain reversal, Uchida-Ikeda model is modified to distinguish 90° domain reversal and 180° domain reversal based on their charge contributions. According to the model, it is estimated that 180°

and 90° domain reversals account for 29% and 71%, respectively, in a sufficiently poled ceramic sample, which coincides well with the result observed by domain-reversal-induced charge.

Based on the quantitative study of 90° domain via XRD measurement, BS-PT ceramics are proved to have a high-temperature stability and its piezoelectric constant remains as high as 95% of its initial value after depoling at 200 °C, which is supported by the insignificant 90° domain reversal percentage of 5%. The insight into domain evolution of tetragonal BS-PT piezoelectric ceramics during electric poling and thermal depoling provides us with a better understanding of the relation between piezoelectricity and domain structure, which is also of heuristic significance to other perovskite piezoelectric ceramics.

Acknowledgments

Jingen Wu appreciates the support from the Fundamental Research Funds for the Central Universities. This work was supported by the National Natural Science Foundation of China (Grant Nos. 51132001, 51072003), the Beijing Municipal Science and Technology Projects (Grant Nos. Z131100003213020, Z151100003715003), the United States Office of Naval Research (ONR Grants No. N00014-12-1-1045 and N00014-16-1-3106) and the Natural Sciences & Engineering Research Council of Canada (Grant No. 203773).

ORCID

Jingen Wu: 0000-0001-9289-5013

Zuo-Guang Ye: 0000-0003-2378-7304

Shuxiang Dong: 0000-0002-9617-6013

References

[1] A. Roelofs, N. A. Pertsev, R. Waser, F. Schlaphof, L. M. Eng, C. Ganpule, V. Nagarajan and R. Ramesh, *Appl. Phys. Lett.*, 2002, **80**, 1424-1426.

[2] L. Chen, J. Ouyang, C. S. Ganpule, V. Nagarajan, R. Ramesh and A. L. Roytburd, *Appl. Phys. Lett.*, 2004, **84**, 254-256.

[3] C. S. Ganpule, V. Nagarajan, H. Li, A. S. Ogale, D. E. Steinhauer, S. Aggarwal, E. Williams, R. Ramesh and P. De Wolf, *Appl. Phys. Lett.*, 2000, **77**, 292-294.

[4] F. Xu, S. Trolier-McKinstry, W. Ren, B. Xu, Z. L. Xie and K. J. Hemker, *J. Appl. Phys.*, 2001, **89**, 1336-1348.

[5] N. Setter, D. Damjanovic, L. Eng, G. Fox, S. Gevorgian, S. Hong, A. Kingon, H. Kohlstedt, N. Y. Park, G. B. Stephenson, I. Stolitchnov, A. K. Taganstev, D. V. Taylor, T. Yamada and S. Streiffer, *J. Appl. Phys.*, 2006, **100**, 51606.

[6] K. Wang and J. Li, *Adv. Funct. Mater.*, 2010, **20**, 1924-1929.

[7] Y. Qin, J. Zhang, Y. Gao, Y. Tan and C. Wang, *J. Appl. Phys.*, 2013, **113**, 204107.

[8] Y. Qin, J. Zhang, Y. Tan, W. Yao, C. Wang and S. Zhang, *J. Eur. Ceram. Soc.*, 2014, **34**, 4177-4184.

[9] G. Arlt and P. Sasko, *J. Appl. Phys.*, 1980, **51**, 4956-4960.

[10] R. E. Eitel, C. A. Randall, T. R. Shrout and S. Park, *Jpn. J. Appl. Phys.*, 2002, **41**, 2099-2104.

[11] R. E. Eitel, S. J. Zhang, T. R. Shrout, C. A. Randall and I. Levin, *J. Appl. Phys.*, 2004, **96**, 2828-2831.

[12] X. Li, J. Chen, Z. Chen and S. Dong, *Appl. Phys. Lett.*, 2012, **101**, 72902.

[13] J. Chen, Z. Chen, X. Li and S. Dong, *Appl. Phys. Lett.*, 2013, **102**, 52902.

[14] J. Chen, X. Li, G. Liu, Z. Chen and S. Dong, *Appl. Phys. Lett.*, 2012, **101**, 12909.

[15] J. Wu, X. Chen, Z. Chu, W. Shi, Y. Yu and S. Dong, *Appl. Phys. Lett.*, 2016, **109**, 173901.

[16] J. Wu, H. Shi, T. Zhao, Y. Yu and S. Dong, *Adv. Funct. Mater.*, 2016, **26**, 7186-7194.

[17] J. Íñiguez, D. Vanderbilt and L. Bellaiche, *Phys. Rev. B*, 2003, **67**, 224107.

[18] J. L. Jones, E. Aksel, G. Tutuncu, T. Usher, J. Chen, X. Xing and A. J. Studer, *Phys. Rev. B*, 2012, **86**, 024104.

[19] K. V. Lalitha, A. N. Fitch and R. Ranjan, *Phys. Rev. B*, 2013, **87**, 064106.

[20] J. Wu, X. Gao, Y. Yu, J. Yang and S. Dong, *J. Alloy Compd.*, 2018, **745**, 669-676.

[21] T.-L. Zhao, A. A. Bokov, J. Wu, H. Wang, C.-M. Wang, Y. Yu, C.-L. Wang, K. Zeng, Z.-G. Ye and S. Dong, *Adv. Funct. Mater.,* 2019, **1807920**, 1-10.

[22] J. Wu, Y. Yu, X. Li, X. Gao and S. Dong, *J. Am. Ceram. Soc.*, 2015, **98**, 3145-3152.

[23] S. J. Zhang, E. F. Alberta, R. E. Eitel, C. A. Randall and T. R. Shrout, *IEEE T. Ultrason. Ferr.*, 2005, **52**, 2131-2139.

[24] Y. Qin, J. Zhang, W. Yao, C. Wang and S. Zhang, *J. Am. Ceram. Soc.*, 2015, **98**, 1027-1033.

[25] F. X. Li and R. K. N. D. Rajapakse, *J. Appl. Phys.*, 2007, **101**, 54110.

[26] Y. Li, Y. Sun and F. Li, *Ceram. Int.*, 2013, **39**, 8605-8614.

[27] N. Uchida and T. Ikeda, *Jpn. J. Appl. Phys.*, 1967, **6**, 1079-1088.

[28] L. K. V., C. M. Fancher, J. L. Jones and R. Ranjan, *Appl. Phys. Lett.*, 2015, **107**, 52901.

[29] J. L. Jones, E. B. Slamovich and K. J. Bowman, *J. Appl. Phys.*, 2005, **97**, 34113.

[30] Y. Saito, *Jpn. J. Appl. Phys.*, 1997, **36**, 5963-5969.
[31] S. Li, A. S. Bhalla, R. E. Newham and L. E. Cross, *J. Mater. Sci.*, 1994, **29**, 1290-1294.
[32] Y. W. Li *and* F. X. Li, *Mech. Mater.,* 2016, **93**, 246-256.
[33] C. S. *Ganpule*, V. Nagarajan, H. Li, A. S. Ogale, D. E. Steinhauer, S. Aggarwal, E. Williams and R. Ramesh, *Appl. Phys. Lett.*, 2000, **77**, 292.
[34] J. L. Jones and M. H. E. D. J. Studer, *Appl. Phys. Lett.*, 2006, **89**, 092901.
[35] C. Bedaya, C. Muller, J. L. Baudour, V. Madigou, M. Anne and M. Roubin, *Mat. Sci. Eng. B,* 2000, **75**, 43-52.
[36] X. Zhang, C. Lei and K. Chen, *J. Am. Ceram. Soc.*, 2005, **88**, 335-338.
[37] H. Yan, H. Zhang and M. J. Reecea, *Appl. Phys. Lett.*, 2005, **87**, 082911.
[38] S. Chen, X. Dong, C. Mao and F. Cao, *J. Am. Ceram. Soc.*, 2006, **89**, 3270-3272.
[39] T. Y. Ansell, D. P. Cann, E. Sapper and J. Rödel, *J. Am. Ceram. Soc.*, 2015, **98**, 455-463.
[40] Y. Wang, K. Cai, T. Shao, Q. Zhao and D. Guo, *J. Appl. Phys.*, 2015, **117**, 164102.
[41] C. Huang, K. Cai, Y. Wang, Y. Bai and D. Guo, *J. Mat. Chem. C*, 2018, **6**, 1433-1444.
[42] J. Chen, G. Liu, X. Li, Z. Chen and S. Dong, *IEEE T. Ultrason. Ferr.*, 2013, **60**, 446-450.

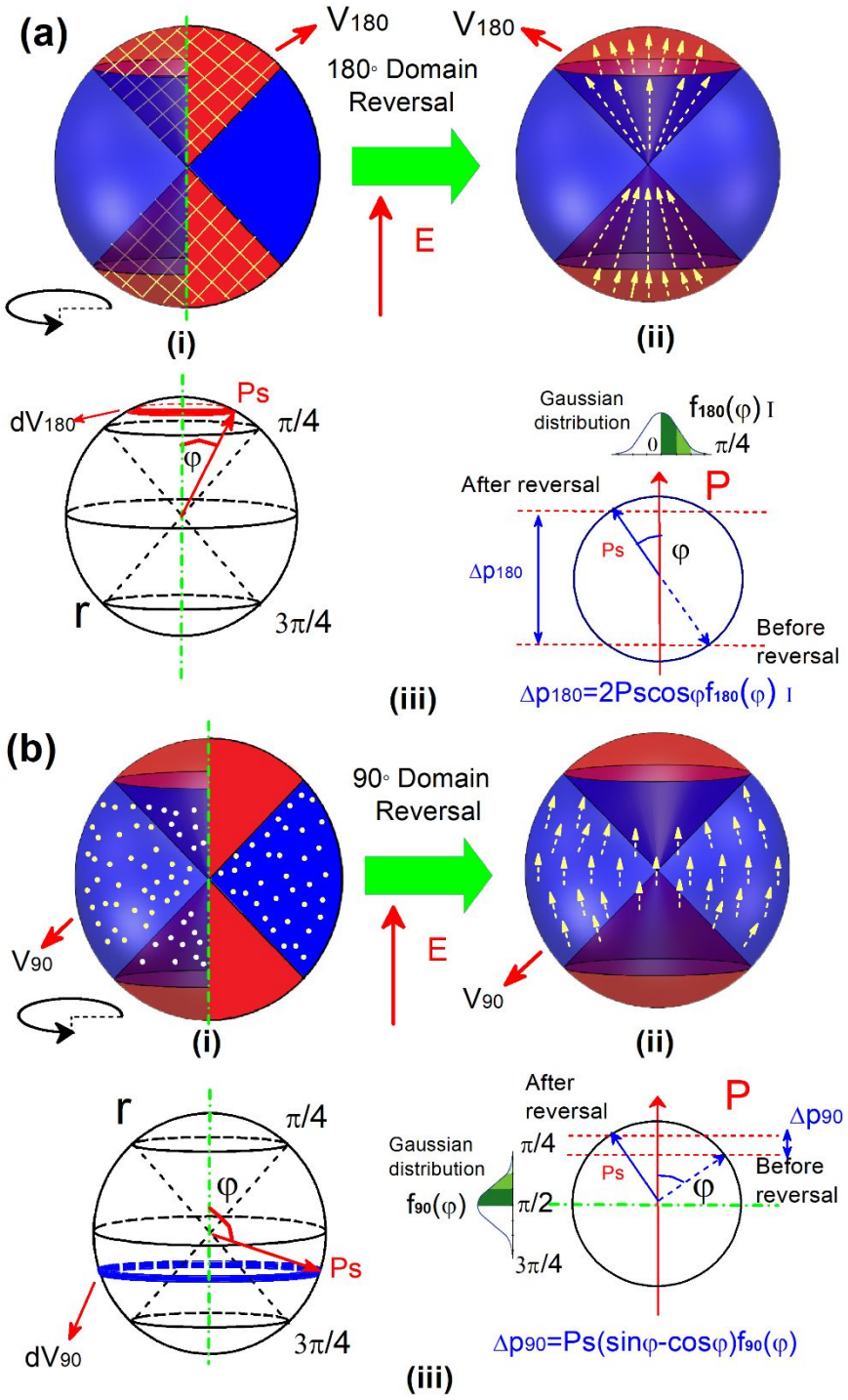

Fig. 1 (a) schematics of 180° domain reversal in electric poling process, (b) schematics of 90° domain reversal in electric poling process. Here, both 180° and 90° reversed dipoles are assumed to obey the Gaussian distribution with respect to their spatial angle φ. $f_{180}(\varphi)$ (including $f_{180}(\varphi)_I$ and $f_{180}(\varphi)_{II}$) and $f_{90}(\varphi)$ are the Gaussian probability distribution functions of the 180° and 90° reversed dipoles, respectively.

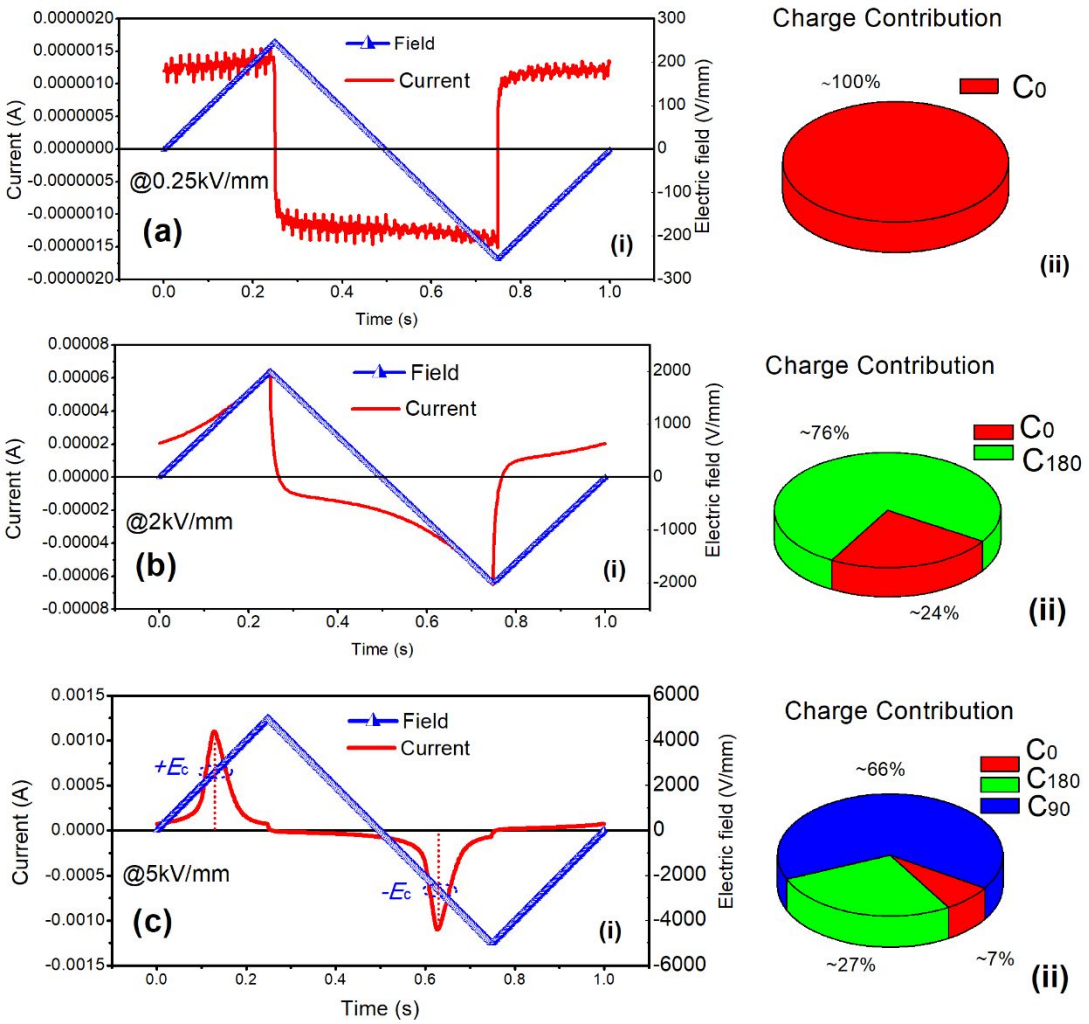

Fig. 2 Switching currents and charge contributions of capacity stored charge (Q_{C_0}), 180° domain reversal induced charge (Q_{180}) and 90° domain reversal induced charge (Q_{90}) under: (a) low (0.25 kV/mm), (b) medium (2 kV/mm), and (c) high (5 kV/mm) poling electric fields. All the measurements were performed at room temperature under 1 Hz.

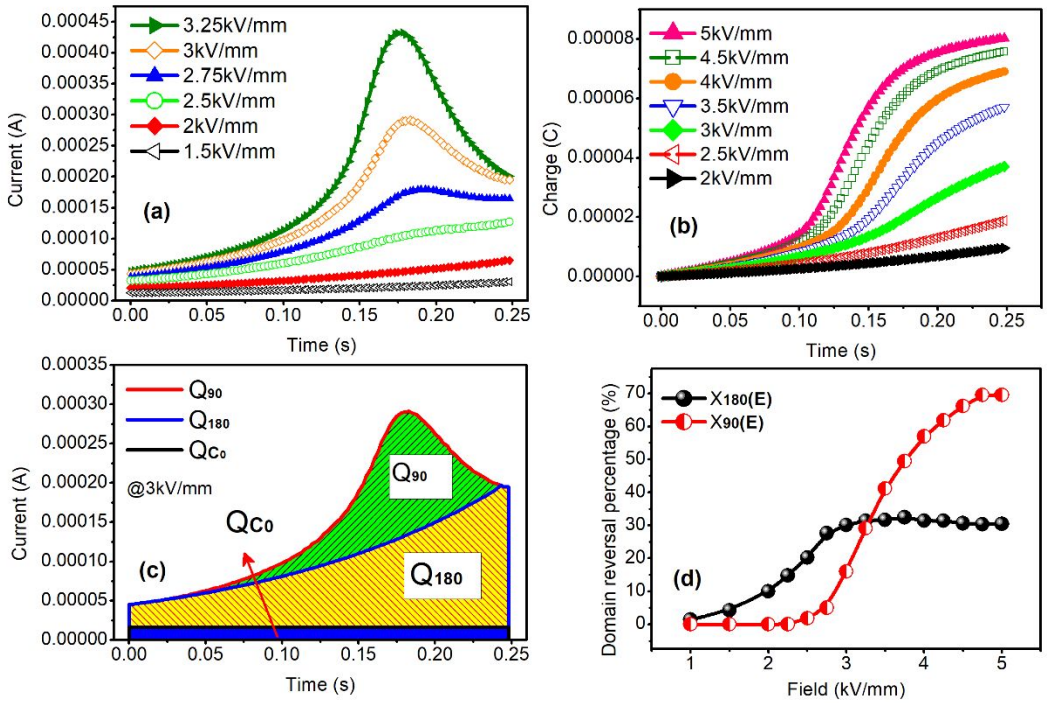

Fig. 3 (a) time dependence of switching current obtained from BS-PT ceramic sample under different poling fields; (b) time dependence of the total induced charge under different poling fields; (c) time dependence of switching current induced by capacity stored charge (Q_{C_0}), 180° domain reversal induced charge (Q_{180}) and 90° domain reversal induced charge (Q_{90}) under the poling filed of 3 kV/mm; (d) field dependence of 180° domain reversal percentage (X_{180}) and 90° domain reversal percentage (X_{90}). All the measurements were performed at room temperature under 1 Hz.

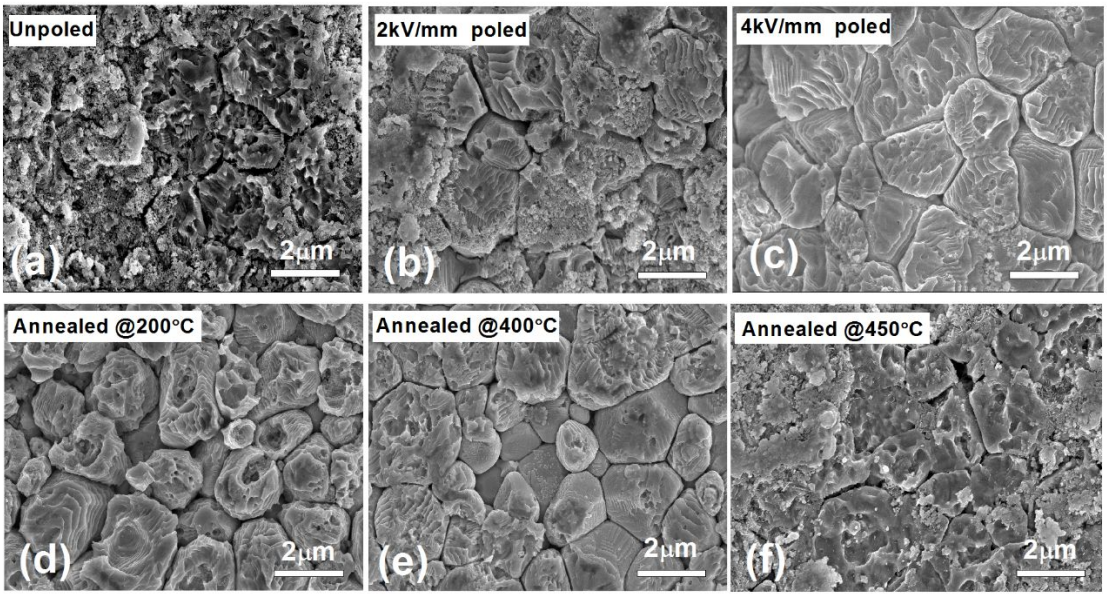

Fig. 4 SEM images of domain microtopography for BS-PT ceramic samples: (a) unpoled; (b) poled at 2 kV/mm; (c) poled at 4 kV/mm; (d) annealed at 200 ºC for 1h; (e) annealed at 400 ºC for 1h; (f) annealed at 450 ºC for 1h.

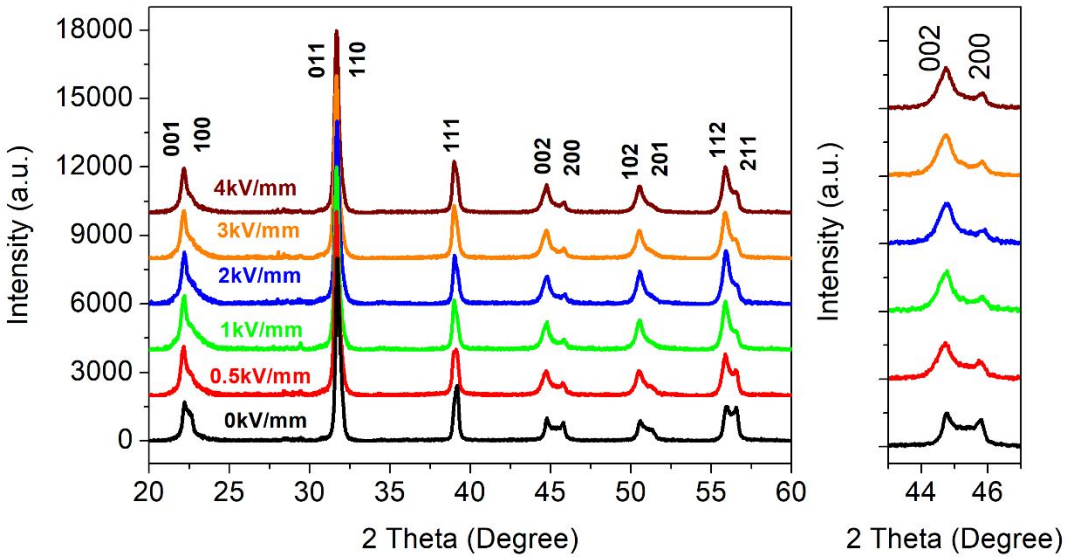

Fig. 5 XRD patterns in the 2 theta range of 20° to 60° for BS-PT ceramic samples poled under different electric fields. The enlarged XRD patterns in the 2 theta range of 43° to 47° are also presented.

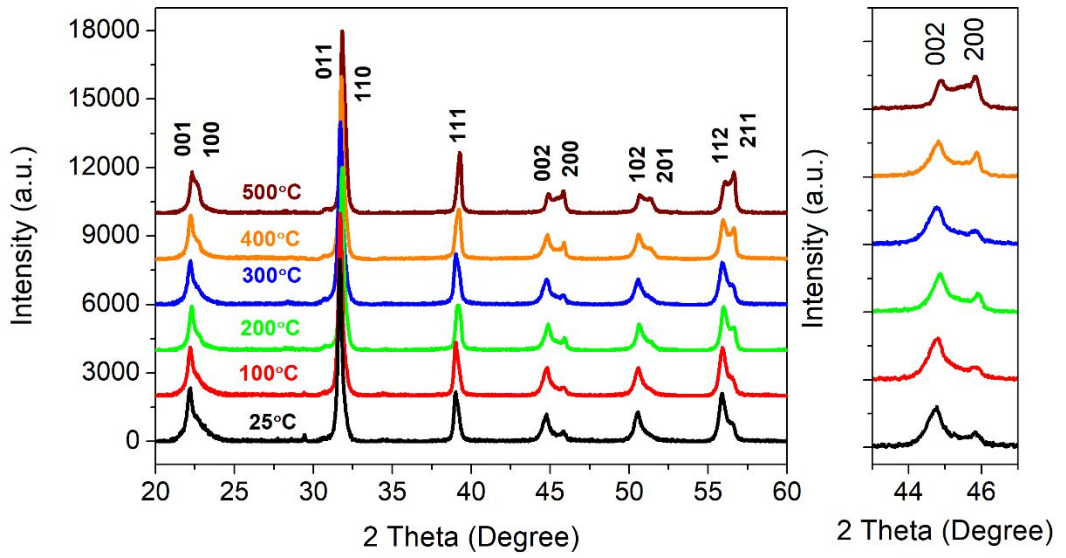

Fig. 6 XRD patterns in the 2 theta range of 20° to 60° for BS-PT ceramic samples thermally depoled under different annealing temperatures. The enlarged XRD patterns in the 2 theta range of 43° to 47° are also presented.

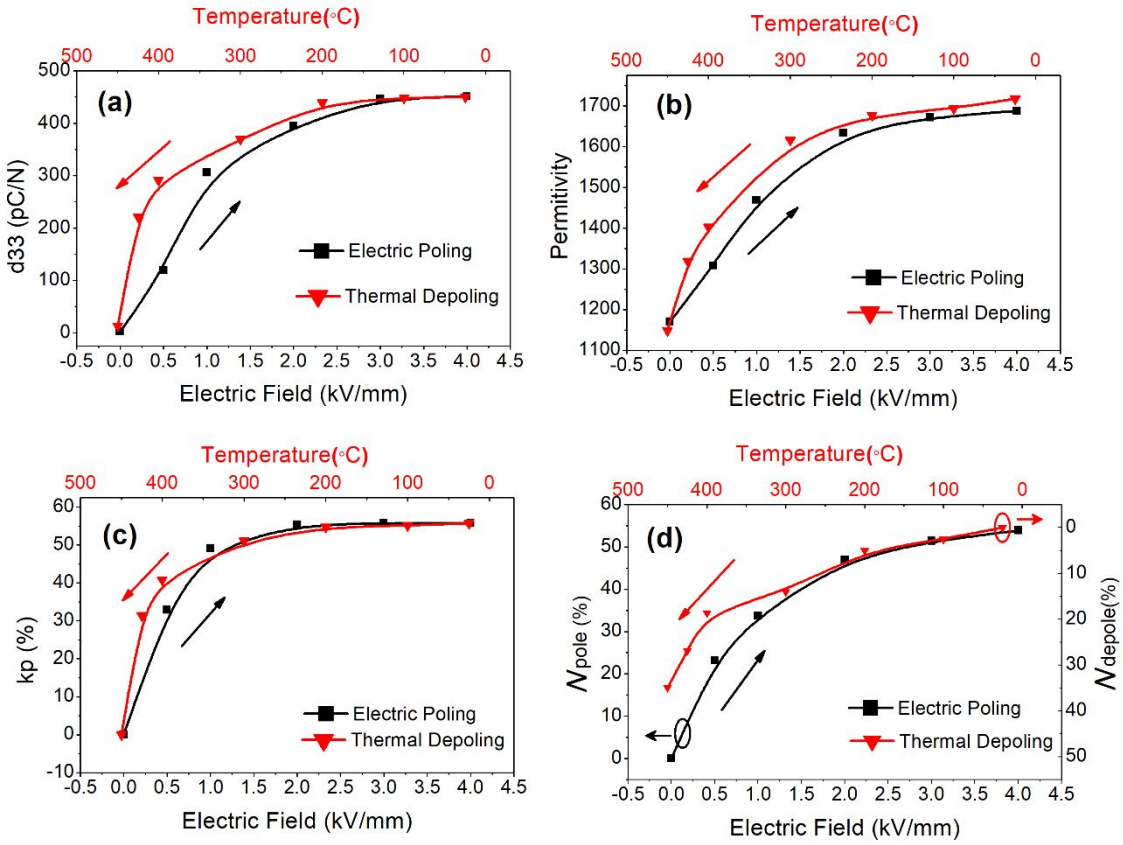

Fig. 7 The effects of electric poling and thermal depoling on the material properties of BS-PT ceramic: (a) piezoelectric constant d_{33}, (b) relative permittivity ε_r, (c) electromechanical coupling factor k_p, (d) N_{pole} and N_{depole} domain reversal percentages.